O'Neill, George C. and Barratt, Eleanor L. and Hunt, Benjamin A. E. and Tewarie, Prejaas K. and Brookes, Matthew Jon (2015) Measuring electrophysiological connectivity by power envelope correlation: a technical review on MEG methods. Physics in Medicine and Biology, 60 (21). R271-R295. ISSN 1361-6560

Measuring electrophysiological connectivity by power envelope correlation: A technical review on MEG methods

George C. O'Neill[1], *Eleanor L. Barratt*[1], *Benjamin A.E. Hunt*[1], *Prejaas K. Tewarie*[1], *and Matthew J. Brookes*[1*]

[1] Sir Peter Mansfield Imaging Centre, School of Physics and Astronomy, University of Nottingham, Nottingham, UK.

*Corresponding author:
Matthew J. Brookes
Sir Peter Mansfield Imaging Centre
School of Physics and Astronomy
University of Nottingham
University Park
Nottingham
Email: matthew.brookes@nottingham.ac.uk
Tel: 0115 9515188

Key words: Magnetoencephalography; MEG; functional connectivity; networks; beamformer; Hilbert envelope; leakage; electrophysiology

Page count: 33
Word count: 13,380 (inc. references and captions)
Figures: 7
References: 121

Running Title: Functional Connectivity Analysis in MEG

ABSTRACT

The human brain can be divided into multiple areas, each responsible for different aspects of behaviour. Healthy brain function relies upon efficient connectivity between these areas and, in recent years, neuroimaging has been revolutionised by an ability to estimate this connectivity. In this paper we discuss measurement of network connectivity using magnetoencephalography (MEG), a technique capable of imaging electrophysiological brain activity with good (~5mm) spatial resolution and excellent (~1ms) temporal resolution. The rich information content of MEG facilitates many disparate measures of connectivity between spatially separate regions and in this paper we discuss a single metric known as power envelope correlation. We review in detail the methodology required to measure power envelope correlation including i) projection of MEG data into source space, ii) removing confounds introduced by the MEG inverse problem and iii) estimation of connectivity itself. In this way, we aim to provide researchers with a description of the key steps required to assess envelope based functional networks, which are thought to represent an intrinsic mode of coupling in the human brain. We highlight the principal findings of the techniques discussed, and furthermore, we show evidence that this method can probe how the brain forms and dissolves multiple transient networks on a rapid timescale in order to support current processing demand. Overall, power envelope correlation offers a unique and verifiable means to gain novel insights into network coordination and is proving to be of significant value in elucidating the neural dynamics of the human connectome in health and disease.

1) INTRODUCTION:

Magnetoencephalography (MEG; Cohen, 1968, 1972) is a non-invasive technique to image electrical activity in the human brain, based upon assessment of the changes in magnetic field induced by synchronised neural current flow. These magnetic fields are of order ~10^{-14} T in magnitude, but are detectable using superconducting quantum interference devices (SQUIDs; Zimmerman *et al.*, 1970; Hämäläinen *et al.*, 1993). The fundamental principle is to place an array of detectors around the head and measure moment-to-moment changes in the spatial topography of the extra-cranial magnetic fields. Appropriate mathematical modelling of these field data facilitates reconstruction of a set of 3-dimensional current density images, which depict spatio-temporal changes in neuro-electrical activity across the brain volume, while a subject undertakes some mental task. The last decade has seen MEG technology 'come of age'; this is in part fuelled by improved hardware (modern MEG systems now allow whole head coverage with in excess of 300 detectors). However, equally important has been a marked improvement in the utility of modelling algorithms that are available to mathematically model MEG data, and a rapid enhancement of computer processing power, which is required to deal with the vast data generated. MEG systems, alongside advanced modelling strategies, now facilitate metrics of brain activity with unprecedented spatiotemporal accuracy, which are allowing novel insights into human brain function in health and disease. The data recorded by MEG systems are dominated by "neural oscillations", which comprise periodic signals in the 1-200 Hz frequency range and are generated by rhythmic electrical activity synchronised across neuronal assemblies. Oscillatory effects of this nature were first reported by Berger in 1924 (Berger, 1929), who measured the electric field at the scalp surface and noted the existence of an 8-13 Hz "alpha" rhythm. Further prominent frequency ranges have since been identified including the delta (1-4 Hz), theta (4-8 Hz), beta (13-30 Hz) and gamma (30-200 Hz) bands. These spontaneous rhythms are present even when the brain is apparently at rest (i.e. when a subject is asked to "do nothing"). For many years such effects were considered "brain noise" with little or no relevance to neural computation. However more recently it has been suggested that oscillations may play an important role in co-ordinating brain activity, with subtle and focal changes in oscillatory dynamics being linked to stimulus presentation (Stevenson *et al.*, 2011), attentional shifts (Bauer *et al.*, 2014) and task performance (Puts *et al.*, 2011).

Recent years have seen a paradigm shift in functional neuroimaging following the discovery that spontaneous brain "activity" (i.e. brain activity recorded when a subject isn't apparently doing anything) contains meaningful spatio-temporal structure. The first demonstrations of such structure were generated using functional magnetic resonance imaging (fMRI; Biswal *et al.*, 1995) and

positron emission tomography (PET; Raichle *et al.*, 2001) The primary finding showed that, even in the absence of a task, brain activity measured in spatially separate, functionally specific, regions exhibits temporal correlation. Such statistical interdependencies, now termed functional connectivity, allowed for elucidation of spatial patterns showing networks of brain regions that appear to work in concert. The principal observation is that the brain contains a relatively small set of "resting state networks" (RSNs). Some RSNs are associated with sensory processing (e.g. the visual or sensorimotor networks) whilst others appear to support attention and cognition (e.g. the dorsal attention or default mode networks). What is clear is that these patterns are important for healthy brain function and abnormal in disease. RSN structure and function has been predominantly investigated using fMRI. However the link between neural oscillations and co-ordination of brain activity led a number of groups to hypothesise that neural oscillations are an intrinsic mode of electrophysiological coupling between regions (Schnitzler and Gross, 2005; Schoffelen and Gross, 2009; Engel *et al.*, 2013). Indeed, MEG based assessment of functional connectivity has been achieved by a number of groups, based upon measurement of oscillations (Tass *et al.*, 1998; Ioannides *et al.*, 2000; Gross *et al.*, 2001; Gross *et al.*, 2002; Jerbi *et al.*, 2007; Gow *et al.*, 2008; Brookes *et al.*, 2011b; Hipp *et al.*, 2012; Brookes *et al.*, 2012a; Luckhoo *et al.*, 2012; Marzetti *et al.*, 2013; Tewarie *et al.*, 2013; Baker *et al.*, 2014; O'Neill *et al.*, 2015). The high information content of MEG signals means that functional connectivity can be derived in many different ways (see Scholvinck *et al.*, 2013 for a review) and whilst a number of types of coupling have become prominent, two in particular have become popular. The first arises from a fixed phase relationship between band-limited oscillatory signals (i.e. phase synchronisation); the second is the result of synchronisation between the amplitude envelopes of band limited oscillations (see Figure 1). Envelope based coupling has shown that spatial patterns, with similar topography to fMRI based RSNs, can be generated using MEG - this finding has now been verified by a number of groups (Liu *et al.*, 2010; de Pasquale *et al.*, 2010; Brookes *et al.*, 2011a; Brookes *et al.*, 2011b; Hipp *et al.*, 2012; Luckhoo *et al.*, 2012; Brookes *et al.*, 2012a; Hall *et al.*, 2014; Hall *et al.*, 2013; Wens *et al.*, 2014a; Hipp and Siegel, 2015).

MEG has distinct advantages for the characterisation of RSNs when compared to other imaging methods. Firstly, by assessing electrophysiological changes, MEG facilitates a more direct inference on neuro-electrical processes compared with modalities such as fMRI, which measure only metabolic consequences of electrical activity. This is particularly important given the evidence that neural oscillations might represent an intrinsic physiological process by which connectivity is mediated. Secondly, the richness of the MEG signal offers the potential to uncover a hierarchy of

functional connections across a range of spatial and temporal scales; these include the phase and envelope connectivity metrics mentioned above which may occur within different frequency ranges, and also cross frequency (Florin and Baillet, 2015) and nonlinear (Wibral *et al.*, 2014) coupling mechanisms. Finally, a shift in connectivity research towards assessment of transient coupling (Hutchison *et al.*, 2013) (i.e. functional networks that form and dissolve over short (even sub-second) time frames) means that MEG, which exhibits millisecond temporal resolution, offers natural advantages over fMRI where the measured blood oxygenation level dependent (BOLD) haemodynamic signal has a temporal resolution of around 5 s. These arguments, coupled with good spatial resolution of MEG, which can be 5mm or better in brain regions with a high signal to noise ratio (SNR) (Troebinger *et al.*, 2014), suggest that it should be a method of choice for investigation of the human connectome. However, a number of significant technical challenges exist, in particular the MEG inverse problem (inferring 3D distributions of moment to moment change in neural current based only on extra cranial magnetic fields) is ill posed (Hadamard, 1902). This means that estimated timecourses of brain current at spatially separate regions are not necessarily independent. As a result, estimated functional connectivity between regions can be artefactually inflated. This significant confound makes connectivity modelling using MEG non-trivial.

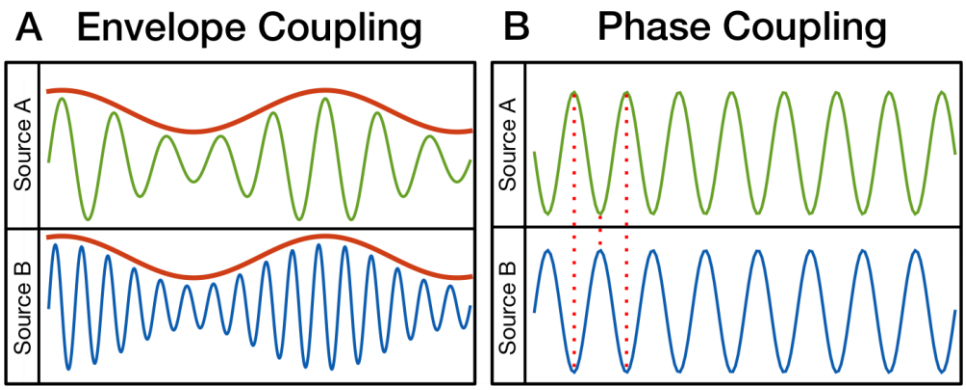

Figure 1: Schematic diagram of phase and envelope based connectivity analyses based upon neural oscillations. A) Envelope coupling is based upon correlation between the oscillatory envelopes of two band limited sources. B) Phase coupling seeks a constant phase lag between signals, in this case a difference of π.

In this article, we aim to provide a technical review on the use of MEG as a way to quantify functional connectivity in the human brain. We choose to focus our article on envelope correlation since i) it exhibits close correspondence with fMRI based RSNs and ii) phase based measurements have been reviewed previously (Schnitzler and Gross, 2005; Scholvinck *et al.*, 2013; Engel *et al.*, 2013). The reader should note however that in focussing on envelope methods we do not undermine the importance of phase based coupling metrics. It is also worth noting that whilst we

focus on MEG, the methodology here is (in theory) compatible with electroencephalography (EEG). In what follows, section 2 introduces the advantages of source space modelling over sensor space methods and describes mathematical means by which source space projection is achieved. Section 3 introduces the problems of artefactual connectivity generated as a result of the inverse problem, and section 4 discusses possible solutions. Section 5 reviews current literature on envelope based networks in MEG and their concordance with other imaging modalities. Finally, section 6 shows how MEG allows insight into rapidly evolving network dynamics.

2) FROM SENSOR TO SOURCE SPACE

The magnetic fields that form the basis of MEG are measured using ~300 discrete detectors placed ~2cm from the scalp surface. It is possible to undertake functional connectivity analysis in "sensor space" via assessment of correlation between signals measured at separate detectors. However, this comes with two distinct disadvantages:

i) **Field spread:** The spatial extent of magnetic fields around a current dipole means that multiple sensors will detect signals from a single source (analogous to volume conduction in EEG). This is well known (Nunez and Srinivasan, 2006; Schoffelen and Gross, 2009b) and means that a single MEG sensor records a complex mixture of signals generated by many sources, making connectivity assessment between sensors difficult to interpret (see Figure 2A).

ii) **Interference:** The magnetic fields generated by the brain are smaller than those generated by external environmental interference (e.g. 50/60 Hz mains electricity). In addition, biological interference, for example from the heart, is larger than the neuromagnetic fields of interest. Interference typically affects many MEG sensors, and hence is highly likely to artificially increase functional connectivity which is calculated as statistical dependency between sensors.

The limitations with sensor space analysis are well documented (Schoffelen and Gross, 2009). Whilst highly successful and meaningful connectivity analyses have been undertaken in this way (Stam, 2004; Bassett *et al.*, 2006; Liu *et al.*, 2010), the inference is usually based on a global parameter (i.e. an integrated measure of global connectivity collapsed across all possible sensor pairs). This means that sensor analysis provides only limited means of interpreting precisely which brain regions or networks are involved.

The most successful means to ameliorate the confounds of sensor based connectivity analysis is to apply source space modelling (Schoffelen and Gross, 2009). This essentially involves mathematically

reconstructing the timecourses of electrical activity across many locations (voxels (Hipp *et al.*, 2012) or parcellated regions (Tewarie *et al.*, 2014b)) in the brain prior to assessment of connectivity between signals reconstructed at those locations. As noted in our introduction, there has been rapid progress in this area over recent years and, despite the fact that this projection is mathematically ill posed, there now exists verifiable ways by which to achieve accurate spatial localisation of neural sources. These methods have been reviewed at length in previous papers (Hillebrand *et al.*, 2005; Greenblatt *et al.*, 2005; Sekihara and Nagarajan, 2008); here we describe a single framework known as beamforming, that has become popular for use with MEG connectivity measurements (Van Drongelen *et al.*, 1996; Van Veen *et al.*, 1997; Robinson and Vrba, 1998; Gross *et al.*, 2001; Brookes *et al.*, 2008).

Beamforming is a spatial filtering approach to inverse modelling. The electrical activity, $\hat{q}_{\boldsymbol{\theta}}(t)$, for a given dipole location and orientation, $\boldsymbol{\theta}$, somewhere in the brain, is estimated as a weighted sum of the magnetic field data, $\boldsymbol{b}(t)$. If $\boldsymbol{b}(t)$ is an $N \times 1$ vector of magnetic field measurements recorded at all *N* MEG sensors at time *t,* then mathematically,

$$\hat{Q}_{\boldsymbol{\theta}}(t) = \boldsymbol{w}_{\boldsymbol{\theta}}^T \boldsymbol{b}(t), \quad (1)$$

where $\boldsymbol{w}_{\boldsymbol{\theta}}$ represents an $N \times 1$ vector of weighting parameters tuned to $\boldsymbol{\theta}$. Note that most inverse solutions can be formulated in this way (Sekihara and Nagarajan, 2008), and they differ only in the way the weights, $\boldsymbol{w}_{\boldsymbol{\theta}}$ are derived. In beamforming, the weights are derived based on power minimisation: we spatially filter unwanted signals by minimising the total power in the output signal, with the linear constraint that the power from the target location/orientation, $\boldsymbol{\theta}$, remains. Mathematically:

$$\min_{\boldsymbol{w}_{\boldsymbol{\theta}}} \left[E\langle \hat{Q}_{\boldsymbol{\theta}}^2 \rangle \right] \text{ subject to } \boldsymbol{w}_{\boldsymbol{\theta}}^T \boldsymbol{l}_{\boldsymbol{\theta}} = 1 \quad (2)$$

where $E\langle \hat{Q}_{\boldsymbol{\theta}}^2 \rangle$ is the expectation value of reconstructed power $\hat{Q}_{\boldsymbol{\theta}}^2$. $\boldsymbol{l}_{\boldsymbol{\theta}}$ is known as the forward vector and contains a model of the magnetic fields that would be measured if there was a unit current at $\boldsymbol{\theta}$. The forward vector can be generated analytically using Maxwell's Equations and the linear constraint ($\boldsymbol{w}_{\boldsymbol{\theta}}^T \boldsymbol{l}_{\boldsymbol{\theta}} = 1$, which is a simple consequence of the definition of the forward solution) ensures unit gain at $\boldsymbol{\theta}$. The source power, $E\langle \hat{Q}_{\boldsymbol{\theta}}^2 \rangle = E\langle \boldsymbol{w}_{\boldsymbol{\theta}}^T \langle \boldsymbol{b}(t) \boldsymbol{b}(t)^T \rangle \boldsymbol{w}_{\boldsymbol{\theta}} \rangle$ can be approximated as $E\langle \hat{Q}_{\boldsymbol{\theta}}^2 \rangle = \boldsymbol{w}_{\boldsymbol{\theta}}^T \boldsymbol{C}\, \boldsymbol{w}_{\boldsymbol{\theta}}$, where $\boldsymbol{C}$ represents the *N x N* data covariance matrix, whose ij^{th} element indexes the covariance between channels i and j. Equation 2 can be rewritten,

$$\min_{\boldsymbol{w}_{\boldsymbol{\theta}}} \left[\boldsymbol{w}_{\boldsymbol{\theta}}^T \boldsymbol{C}\, \boldsymbol{w}_{\boldsymbol{\theta}} \right] \text{ subject to } \boldsymbol{w}_{\boldsymbol{\theta}}^T \boldsymbol{l}_{\boldsymbol{\theta}} = 1, \quad (3)$$

which can be solved to give

$$\boldsymbol{w}_{\boldsymbol{\theta}}^T = \frac{\boldsymbol{l}_{\boldsymbol{\theta}}^T \boldsymbol{C}^{-1}}{\boldsymbol{l}_{\boldsymbol{\theta}}^T \boldsymbol{C}^{-1} \boldsymbol{l}_{\boldsymbol{\theta}}}. \quad (4)$$

Sequential application of Equations 1 and 4 to all locations and orientations of interest in the brain allows for reconstruction of timecourses of electrical activity at those locations. Subsequent calculation of connectivity between regional timecourses can then be undertaken.

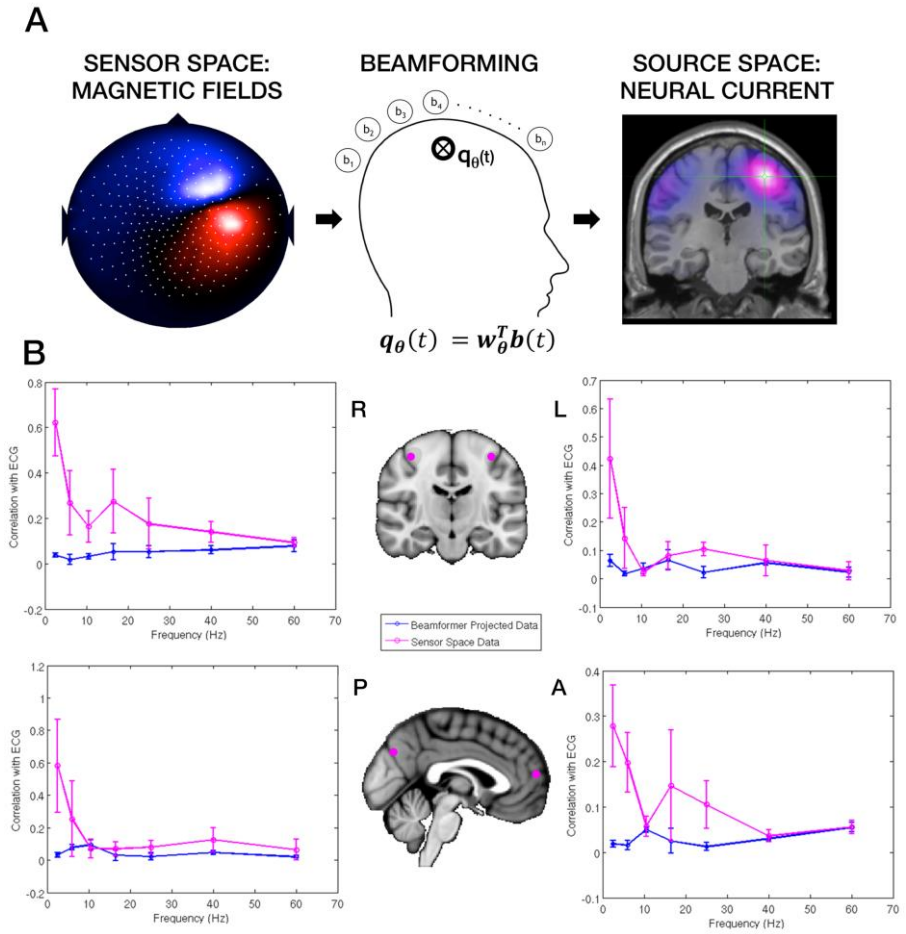

Figure 2: Beamforming. A) Schematic diagram showing the fundamental principle of beamforming. The left hand plot shows a set of sensor space magnetic fields which can be turned into source space estimates of neural current via application of the beamformer algorithm. B) An example of interference rejection by beamforming. The four plots show correlation between the measured electrocardiogram and MEG data. The pink lines show correlation at the sensor level whereas the blue lines show correlation at the source level. The separate plots show different brain locations – the source space analysis was undertaken at brain locations indicated by the red markers. The sensor space analysis at the 5 nearest sensors with the largest magnitude forward vectors for a ROI. Note the excellent reduction in cardiac interference afforded by beamforming.

Source localisation, in part, overcomes the limitations of sensor space measurements. Firstly, it allows results to be formed in source space and overlaid directly onto structural brain images, thus allowing direct interpretation of connectivity with respect to anatomy (see Figure 2A). Secondly, source space projection offers an improved signal to noise ratio: this is true of all source localisation algorithms, but beamforming is particularly efficient at rejecting interference (Sekihara *et al.*, 2001;

Sekihara *et al.*, 2006). At a basic level, the spatial topography of interference does not resemble the spatial topography of a neural source. The minimisation term in Equations 2 and 3 acts to minimise all signals other than those exhibiting a specific source pattern, $\boldsymbol{l_\theta}$. This means that the artefacts with spatial topographies orthogonal to $\boldsymbol{l_\theta}$ can be supressed significantly.

Figure 2B shows an example of interference rejection via beamforming. Here, 600 s of MEG data have been recorded from a single subject using a 275 channel CTF MEG system (MISL, Coquitlam, BC, Canada). In addition, the subject's electrocardiogram (ECG) has been recorded concurrently. The magnetic fields generated by the heart are well known to affect MEG data and here the effect of this on sensor space and source space signals has been calculated. The four plots in Figure 2B show correlation between the ECG and MEG data, plotted as a function of frequency. The pink lines show correlation at the sensor level whereas the blue lines show correlation at the source level after reconstruction, via beamforming, at the locations shown by the red markers. The separate plots show the four different locations. Sensor space analysis was undertaken at the 5 sensors corresponding to the largest absolute elements of the forward vectors from the chosen source space locations, with results averaged over sensors. This example shows clearly the effectiveness of beamforming as an interference rejection methodology: frequency filtered MEG data correlates relatively highly at the sensor level with the (equivalently filtered) ECG. This is particularly true in the low (delta and theta) frequency bands where, correlation coefficients are as high as 0.6. However when moving into source space, these correlation coefficients are reduced to < 0.1 across all frequency bands and locations studied. This interference rejection is of significant utility; if common mode signals are allowed to interfere with MEG signals from separate locations, then artefactual connectivity will necessarily result. By reducing this interference, source space estimates of connectivity are likely to be more accurate reflections of true coupling between regions.

It is important to note that although beamforming has been discussed here, other source localisation techniques are available and equally valid for functional connectivity analysis. For example, Minimum Norm Estimators (MNE; (Hamalainen and Ilmoniemi, 1994; Fuchs *et al.*, 1999; Dale *et al.*, 2000; Pascual-Marqui, 2002) have been used extensively and successfully in many connectivity studies (de Pasquale *et al.*, 2010; Palva *et al.*, 2010; Marzetti *et al.*, 2013; Wens *et al.*, 2014b) and in some cases offer advantages over beamforming. Specifically, it is well known that beamforming supresses spatially separate but temporally correlated sources and, in principle, this may confound connectivity metrics. For example, multiple studies have shown that beamforming fails to reconstruct bilateral auditory steady state evoked sources (Dalal *et al.*, 2006; Brookes *et al.*,

2007; Popescu *et al.*, 2008; Diwakar *et al.*, 2011) due to correlation between signals generated in opposite hemispheres. Such a failure in reconstruction would clearly lead to artefactual task induced auditory connectivity estimates, and may also impact upon resting state investigations. In such cases MNE would prove advantageous since it is able to reconstruct correlated sources. This said, it should be noted that for beamformer suppression to take place, zero time lagged correlation must exist between source signals. In fact, zero-time-lag correlated signals potentially reflect source leakage (see below). Therefore it follows that, rather than the beamformer suppression of correlated sources acting as a confound, it may act in a positive way to supress artefacts. (See also section 3: *Signal Leakage in Source Space* for more details).

Although there are subtle advantages and disadvantages to different inverse methodologies, in practice there is similarity between functional networks generated using the same data with different underlying source localisation approaches. Figure 3 shows example results, with functional networks generated using resting state MEG data from 9 subjects (600 seconds of data per subject). Data were frequency filtered in the beta (13-30 Hz) band and sources were reconstructed using both beamformer and MNE at the vertices of an isotropic 8mm grid across the brain. Amplitudes of the signals were calculated, downsampled to 1 Hz, and analysed using temporal independent component analysis (tICA) to generate envelope networks. ICs were matched using Pearson correlation to identify which BF and MNE components were the most similar in time (r_T). Figure 3 shows ICs with the highest r_T values. Results show clear similarity in terms of spatial topography, which is reflected in their high spatial correlations (r_S). This implies that, whilst different inverse methods may offer specific advantages, resulting network patterns can be highly similar.

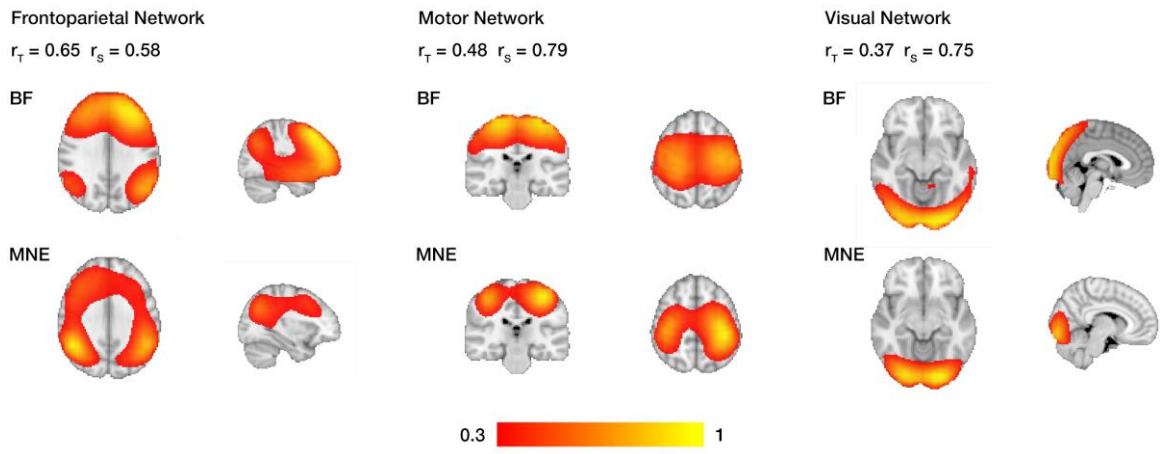

Figure 3: Beamforming and minimum norm derived networks from the same MEG data. Spatial topographies of 3 networks (Visual, Motor and Fronto-Parietal) are shown. Networks were identified using ICA and matched by temporal correlation of IC timecourses (O'Neill et al., 2013). Note the similarity across the two inverse methods.

3) SIGNAL LEAKAGE IN SOURCE SPACE

Despite the advantages of source space estimation, a significant problem remains, which is typically termed “signal leakage”. The ill-posed nature of the MEG inverse problem causes a degree of spatial blurring in source space reconstruction. This means that a single point source will appear to spread across a finite volume. In addition to this spread, it is also possible for sources to be mislocalised, for example due to inaccuracies in modelling the forward vector or deviation from the assumptions driving the inverse model. These effects mean that if two independent sources, whose orthogonal timecourses are described by $\boldsymbol{q}_1$ and $\boldsymbol{q}_2$, are reconstructed via beamforming, the resultant estimated timecourses $\widehat{\boldsymbol{q}}_1$ and $\widehat{\boldsymbol{q}}_2$ may no longer be orthogonal. In other words, signals originating from one brain location can “leak" into the estimated signals from a separate brain region. This can lead to spurious functional connectivity estimates and so it is of significant importance to measure, and if possible eliminate, the likely effects of signal leakage before assessing functional connectivity.

In order to better understand the leakage effect, a simple analytical analysis proves helpful. Consider a case of two sources: $\boldsymbol{q}_1$ is of dimension $1 \times P$ and represents the timecourse from a test location, $\boldsymbol{r}_1$. $\boldsymbol{q}_2$ is also of dimension $1 \times P$ and represents the timecourse at a seed location, $\boldsymbol{r}_2$. P denotes the number of time samples in the data. Assume that $\boldsymbol{q}_1$ and $\boldsymbol{q}_2$ are completely independent sources so that $\frac{1}{P}\boldsymbol{q}_1\boldsymbol{q}_2^T = 0$ (i.e. the covariance calculated between the two sources is zero). If we assume that there are no other electrophysiological sources in the brain, then the $N \times P$ matrix of MEG data can be described as

$$\boldsymbol{m} = \boldsymbol{l}_1\boldsymbol{q}_1 + \boldsymbol{l}_2\boldsymbol{q}_2 + \boldsymbol{e}, \quad (5)$$

where $\boldsymbol{l}_1$ and $\boldsymbol{l}_2$ (both dimension $N \times 1$) represent the forward vectors for sources $\boldsymbol{q}_1$ and $\boldsymbol{q}_2$ respectively. $\boldsymbol{e}$ has dimension $N \times P$ and represents sensor noise. We can now employ a beamformer to reconstruct an estimate of $\boldsymbol{q}_1$. Using Equation 1,

$$\widehat{\boldsymbol{q}}_1 = \boldsymbol{w}_1^T\boldsymbol{m} \quad (6)$$

where $\boldsymbol{w}_1$ represents the beamformer weights vector for location $\boldsymbol{r}_1$. Substituting for the MEG data using Equation 5, and noting the linear constraint for beamformer weights that $\boldsymbol{w}_1^T\boldsymbol{l}_1 = 1$,

$$\widehat{\boldsymbol{q}}_1 = \boldsymbol{w}_1^T\boldsymbol{l}_1\boldsymbol{q}_1 + \boldsymbol{w}_1^T\boldsymbol{l}_2\boldsymbol{q}_2 = \boldsymbol{q}_1 + \boldsymbol{w}_1^T\boldsymbol{l}_2\boldsymbol{q}_2. \quad (7)$$

This means that the beamformer reconstruction for source 1 is only independent of source 2, if $\boldsymbol{w}_1^T\boldsymbol{l}_2 = 0$. A similar argument can be made so that the beamformer reconstruction of source 2 is:

$$\widehat{\boldsymbol{q}}_2 = \boldsymbol{q}_2 + \boldsymbol{w}_2^T\boldsymbol{l}_1\boldsymbol{q}_1. \quad (8)$$

Given that the underlying true sources are independent ($\frac{1}{P}\widehat{\boldsymbol{q}}_1\widehat{\boldsymbol{q}}_2^T = 0$), it follows that an estimate of the source leakage, s, can be generated by calculation of the covariance between reconstructed timecourses (i.e. $s = \frac{1}{P}\widehat{\boldsymbol{q}}_1\widehat{\boldsymbol{q}}_2^T$). Simple substitution of Equations 7 and 8 gives:

$$s = \boldsymbol{w}_2^T\boldsymbol{l}_1\upsilon_1 + \boldsymbol{w}_1^T\boldsymbol{l}_2\upsilon_2 \quad (9)$$

where υ_1 and υ_2 are the variances of $\boldsymbol{q}_1$ and $\boldsymbol{q}_2$ respectively. This analysis shows that, even in a two source simulation, the leakage term will only drop to zero if $\boldsymbol{w}_2^T\boldsymbol{l}_1 = 0$ and $\boldsymbol{w}_1^T\boldsymbol{l}_2 = 0$. In other words, the weights for source 1, and forward vector for source 2 must be orthogonal, and vice versa. It should be noted that this analysis assumes effectively zero noise (i.e. we have ignored $\boldsymbol{e}$ in Equation 5). The addition of sensor level noise will tend to reduce covariance between the beamformer estimated timecourses, and for this reason Equation 9 represents an upper limit on leakage.

It proves instructive to extend this model in simulation. Our simulations were based on a two source model equivalent to that described above. In all cases a seed source ($\boldsymbol{q}_2$) was placed approximately in the right primary sensorimotor cortex. 2781 iterations of the simulation were run, and on each iteration the test source ($\boldsymbol{q}_1$) was simulated in a different voxel. Voxels were placed on an 8 mm cubic grid spanning the entirety of brain space. Dipole orientation was allowed to vary smoothly with position in order to mimic dipole orientations in real MEG data. The source magnitudes were 8 nAm and source timecourses were generated from a beamformer reconstruction of a resting state MEG experiment. Source timecourses were phase randomised (Prichard and Theiler, 1994) so as to have zero correlation between them. The geometry for the simulation was based upon a 275 channel CTF axial gradiometer MEG system (MISL, Coquitlam, BC, Canada) operating in third order synthetic gradiometer configuration. The location of the MEG sensors with respect to brain anatomy was based on a real experimental recording session. Two separate noise models were used, in case 1, sensor noise was drawn from a Gaussian random process (meaning noise was uncorrelated across sensors). In case 2, real MEG noise was employed (where interference is correlated across MEG sensors). This was generated via the recording of 300 s of real MEG data with no subject in the system.

The results of this simulation are shown in Figure 4. Figure 4A shows images of the magnitude of leakage between the seed source, and test sources at all other locations. The upper panels show the analytical case (which reflects an upper limit on leakage based on Equation 9) whereas the lower panels show results from the actual simulation. The left hand panel shows Gaussian sensor noise whereas the right hand panel shows realistic noise. Note that in all cases source leakage is at its worst in brain areas adjacent to the seed. Note also that leakage worsens when using a realistic

noise model. Figure 4B shows equivalent leakage images for shallow (upper panel) and deep (lower panel) grey matter sources. It is clear that source leakage worsens for deeper sources due to their lower signal to noise ratio. Finally in Figure 4C the upper panel shows the relationship between the analytical model in Equation 9, and the actual simulation where the analytical model gives an upper limit on leakage. The lower panel of Figure 4C shows leakage magnitude as a function of Euclidian distance between the seed and test voxels. Note that even sources separated by as much as 5 cm can exhibit a large amount of signal leakage, which would significantly confound any attempt at functional connectivity analysis.

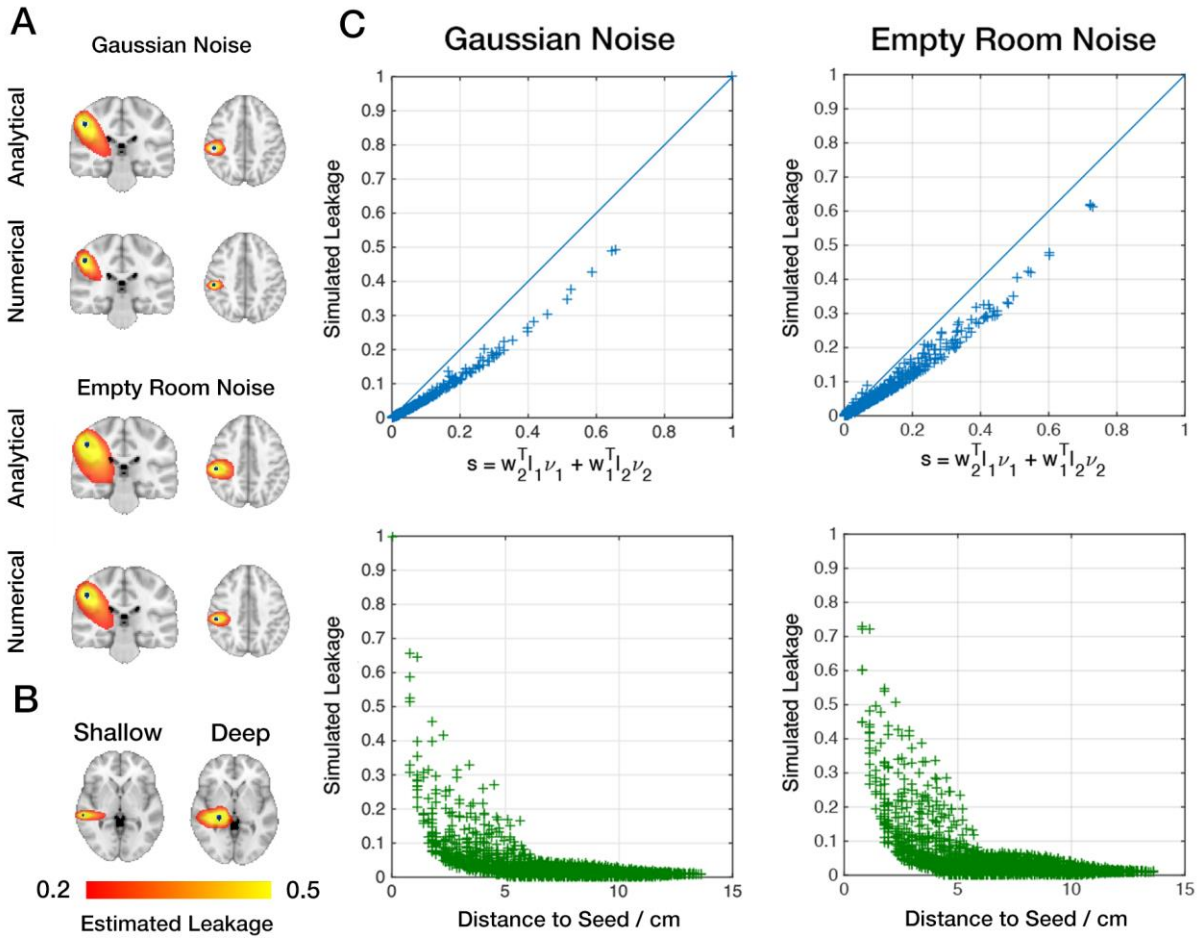

Figure 4: Examples of source space signal leakage. A) Images showing the magnitude of leakage between a simulated source in the primary sensorimotor cortex (blue dot), and equivalent simulated sources placed at all other brain locations. The upper panels show the analytical worst-case scenario whereas the lower panels show results from the actual simulation. The left hand panel shows simulated Gaussian sensor level noise (i.e. the noise is uncorrelated across channels) whereas the right hand panel shows realistic noise (which is correlated across the channels). Note in all cases that source leakage is worst close to the seed and typically spreads asymmetrically around the seed. Note also that leakage worsens with a realistic noise model. B) Equivalent images for a shallow cortical source (upper panel) and a deep source (lower panel); leakage worsens for deeper sources which exhibit a lower signal to noise ratio. C) Upper panel shows the relation between the analytical model in Equation 9, and the actual simulation for every test voxel in the simulation; note the analytical model gives a "worst case scenario" regarding the leakage, which is reduced in the simulation via the addition of sensor level noise. The lower panel shows leakage magnitude as a function of Euclidian distance between the seed and the test voxels.

As shown by the above simulation, signal leakage differs depending on the brain area being studied, the signal to noise ratio of the data and the sensor level noise model. In addition, it depends on the inverse solution being used, and the number of dipoles active in the brain. As can be seen from the images in Figure 4A, the spatial profile of leakage is asymmetric around the seed location.

4) REDUCING SIGNAL LEAKAGE AND CONNECTIVITY ESTIMATION

Leakage reduction

Over the last decade, a number of potential solutions to the source leakage problem have been proposed. Although separate methods have different modes of operation, they are all based on the observation that leakage generates inflated connectivity between estimated sources, which manifests as a zero-phase-lag correlation. Indeed this is shown by Equations 7 and 8, which imply that leakage results in a weighted addition of a distal source. Genuine connectivity, on the other hand, is more likely to incorporate a time lag, generated as electrical signals travel between different brain regions. This means that elimination of *all* zero-phase-lag correlations in source space should result in the elimination of leakage, albeit at the expense of a loss of genuine zero-phase-lag connectivity. As noted above, paradoxically the fact that beamforming supresses temporally correlated sources potentially aids in leakage reduction. However for such suppression to occur, sources must be highly correlated ($r > \sim 0.7$ – which is unlikely for anything other than driven steady state responses) and therefore even after beamforming, further steps must be taken if leakage artefacts are to be reduced. In phase based connectivity metrics (see Figure 1), leakage reduction methods usually circumvent zero-phase (and conversely π-phase) connections by assessing only the imaginary component of coherence between timecourses (Nolte *et al.*, 2004; Nolte *et al.*, 2008; Ewald *et al.*, 2012; Marzetti *et al.*, 2013) or by focusing on the asymmetry of the phase difference distribution (Stam *et al.*, 2007; Vinck *et al.*, 2011). In the current paper, our aim is to focus on envelope based metrics of connectivity. In such cases, different methodologies are employed to remove zero-phase-lag effects (Hipp *et al.*, 2012; Brookes *et al.*, 2012b; Maldjian *et al.*, 2014; Brookes *et al.*, 2014a; Colclough *et al.*, 2015; O'Neill *et al.*, 2015).

Connectivity estimation via envelope correlation traditionally involves first band pass filtering the data to a frequency band of interest. Next, the envelope of the oscillations is generated via some non-linear transform and connectivity between regions is estimated by correlation between envelopes. However, in order to reduce leakage, an extra step must be employed whereby, prior to envelope computation, zero-phase-lag correlations in the underlying signal (i.e. the oscillations themselves) are removed via linear regression. Consider again two beamformer estimated

timecourses $\widehat{\boldsymbol{q}}_1$ and $\widehat{\boldsymbol{q}}_2$, representative of two underlying sources with a linear zero-phase-lag relationship caused by leakage. To mitigate the leakage, we remove a linear projection of the seed voxel, $\widehat{\boldsymbol{q}}_2$, from the test voxel $\widehat{\boldsymbol{q}}_1$. Mathematically we employ a general linear model so that

$$\widehat{\boldsymbol{q}}_{1M} = \widehat{\boldsymbol{q}}_1 - \beta\widehat{\boldsymbol{q}}_2, \quad (10)$$

where β represents the effect size and relates directly to the magnitude of the leakage. $\widehat{\boldsymbol{q}}_{1M}$ is the residual measurement, which represents our leakage-suppressed timecourse for the test location (i.e. $\widehat{\boldsymbol{q}}_{1M}$ is the beamformer estimate of activity in $\widehat{\boldsymbol{q}}_1$, but with any linear dependence on $\widehat{\boldsymbol{q}}_2$ [i.e. leakage] removed). β can be estimated as,

$$\hat{\beta} = \widehat{\boldsymbol{q}}_1\widehat{\boldsymbol{q}}_2^{+}, \quad (11)$$

where the superscript $+$ denotes the Moore-Penrose pseudo-inverse. This method has been employed in several studies (Hipp *et al.*, 2012; Brookes *et al.*, 2012b; Maldjian *et al.*, 2014; O'Neill *et al.*, 2015) with a variety of implementations. One difference between implementations is that some studies assume stationarity (Brookes *et al.*, 2012b), and perform a single leakage correction step for the whole dataset, whereas others propose a dynamic approach correcting small time-windows individually (Hipp *et al.*, 2012; O'Neill *et al.*, 2015). A second difference is that some studies perform leakage reduction between point locations (i.e. $\widehat{\boldsymbol{q}}_1$ and $\widehat{\boldsymbol{q}}_2$ are dimension $1 \times P$), whereas others work in a multivariate framework for cluster based corrections (i.e. $\widehat{\boldsymbol{q}}_1$ and $\widehat{\boldsymbol{q}}_2$ are matrices containing timecourses from multiple voxels within two spatially distinct clusters; (Brookes *et al.*, 2014a)). In all cases, leakage reduction offers significantly improved connectivity estimates compared to uncorrected methods.

Following leakage reduction, there are several ways in which the amplitude envelope of a signal can be found in order to compute connectivity. The most common is the Hilbert transform, which has been well documented in the electrophysiological literature (Tass *et al.*, 1998; Le Van Quyen *et al.*, 2001; Freeman, 2004; Kiebel *et al.*, 2005). Briefly, assuming a source reconstructed timecourse signal $\hat{q}(t)$, then its complex "analytic signal" is given by

$$\hat{z}(t) = \hat{q}(t) + iH[\hat{q}(t)], \quad (12)$$

where H is the Hilbert transform and is defined as,

$$H[\hat{q}(t)] = P\left[\frac{1}{\pi}\int_{-\infty}^{\infty}\frac{\hat{q}(u)}{t-u}du\right]. \quad (13)$$

P is the Cauchy principal value of the integral, which is necessary to account for the singularity which occurs when $t = u$. The signal envelope is then given by

$$E\big(\hat{q}(t)\big) = \sqrt{\big(\hat{q}(t)\big)^2 + (H[\hat{q}(t)])^2}. \quad (14)$$

Note that $E\big(\hat{q}(t)\big)$, is a non-linear and non-reversible transform of $\hat{q}(t)$. The instantaneous phase data contained within $\hat{q}(t)$, which can be obtained directly from the Hilbert transform as $tan(\phi) = H[\hat{q}(t)]/\hat{q}(t)$, is discarded by Equation 14 and is not used on envelope based connectivity metrics. In addition to the band-pass filter and Hilbert transform, there are several alternative methods which could be used, for example the continuous (Morlet) wavelet transform (Le Van Quyen *et al.*, 2001; Kiebel *et al.*, 2005) or the S-transform (Stockwell *et al.*, 1996). Following envelope calculation, connectivity can be estimated simply: if $\boldsymbol{X} = E[\widehat{\boldsymbol{q}}_{1M}]$ is a $1 \times P$ vector representing the envelope of the leakage corrected test source, and likewise $\boldsymbol{Y} = E[\widehat{\boldsymbol{q}}_2]$ is a $1 \times P$ vector representing the envelope of the seed source, connectivity can then be estimated as

$$r(\boldsymbol{X}, \boldsymbol{Y}) = \frac{\boldsymbol{X}\boldsymbol{Y}^T}{\sqrt{\boldsymbol{X}\boldsymbol{X}^T}\sqrt{\boldsymbol{Y}\boldsymbol{Y}^T}}, \quad (15)$$

where $\boldsymbol{X}$ and $\boldsymbol{Y}$ must be mean corrected. Note that Equation 15 simply represents a Pearson correlation coefficient computed between envelopes.

Figure 5A shows an example of envelope based functional connectivity taken from a real MEG recording in a single subject. Five minutes of MEG data were recorded using a 275 channel MEG system (these data were first presented in (Brookes *et al.*, 2012b), and this figure is reproduced with permission). The subject was asked to lie in the system and "think of nothing" whilst connectivity was assessed, over all time, between a seed location in left sensorimotor cortex and all other voxel locations in the brain. In the upper panel, connectivity was computed between the seed and all other test voxels with no leakage reduction applied. In the lower panel, leakage reduction has been employed using the method outlined above. In both cases, envelopes of beta band (13-30 Hz) oscillations were employed. It is clear that a functional network of brain regions exists in the data, with the beta band envelope in left motor cortex showing high levels of correlation with equivalent envelopes in homologous regions of right sensorimotor cortex. In addition, note the significant advantages afforded by the reduction in zero-phase-lag correlation. In the uncorrected case, regions showing high connectivity extend from the seed voxel towards the centre of the brain as well as into the left temporal lobe. The spatial profile of leakage is in good agreement with the simulation presented in Figure 4. This blurring around the seed location is reduced when applying leakage reduction.

Despite the advantages of leakage reduction strategies, they have significant limitations, which should be discussed. Firstly, the regression method does not make the modified test timecourse, $\widehat{\boldsymbol{q}}_{1\mathrm{M}}$, a faithful reconstruction of the true source timecourse $\boldsymbol{q}_1$. In fact, the modified timecourse retains an element of leakage from $\boldsymbol{q}_2$. Only the magnitude of that leakage is altered, in such a way

as to ensure orthogonality between $\widehat{\boldsymbol{q}}_{1\mathrm{M}}$ and $\widehat{\boldsymbol{q}}_2$ (Brookes *et al.*, 2014). Second, as noted above, the method also means the removal of true zero-phase connections; this is significant, particularly given that invasive recordings show significant genuine zero-phase-lag effects in the brain (Singer, 1999). Finally, for the regression method to work, the data need to be Gaussian distributed. This is highlighted in Figure 5B which shows results from a simple simulation. Two signals, $\boldsymbol{X}$ and $\boldsymbol{Y}$, were generated as linear mixtures of independent timecourses, $\boldsymbol{S}_1$ and $\boldsymbol{S}_2$. The first mixture was defined as $\boldsymbol{X} = \boldsymbol{S}_1 - k\boldsymbol{S}_2$ and the second as $\boldsymbol{Y} = \boldsymbol{S}_2 + k\boldsymbol{S}_1$. The parameter k is a positive constant and controls the degree of leakage in the simulation; this was set to 0.2. Three separate simulations were undertaken in which $\boldsymbol{S}_1$ and $\boldsymbol{S}_2$ were drawn from a) Gaussian distributed noise b) leptokurtic noise (Gaussian^3) and c) uniformly distributed platykurtic noise. Leakage reduction was applied to $\boldsymbol{Y}$ and the result should be zero correlation between timecourses following correction. A phase randomisation approach (Prichard and Theiler, 1994) was employed to test the significance of any non-zero correlation observed and the false positive count was calculated as the number of significant measures of correlation observed across 1000 iterations of the simulation. Results show clearly that if the underlying processes ($\boldsymbol{S}_1$ and $\boldsymbol{S}_2$) are normally distributed, the false positive rate (FPR) follows the expected trend (black line). However, if $\boldsymbol{S}_1$ and $\boldsymbol{S}_2$ are either leptokurtic or platykurtic, leakage is poorly accounted for. Overall, the Gaussian assumption is reasonable; indeed it is an assumption at the heart of many of the source localisation methodologies employed in MEG. However situations exist where this is not the case, for example epileptic seizures (Prendergast *et al.*, 2013) and for this reason care should be taken when deploying the regression method to correct for leakage.

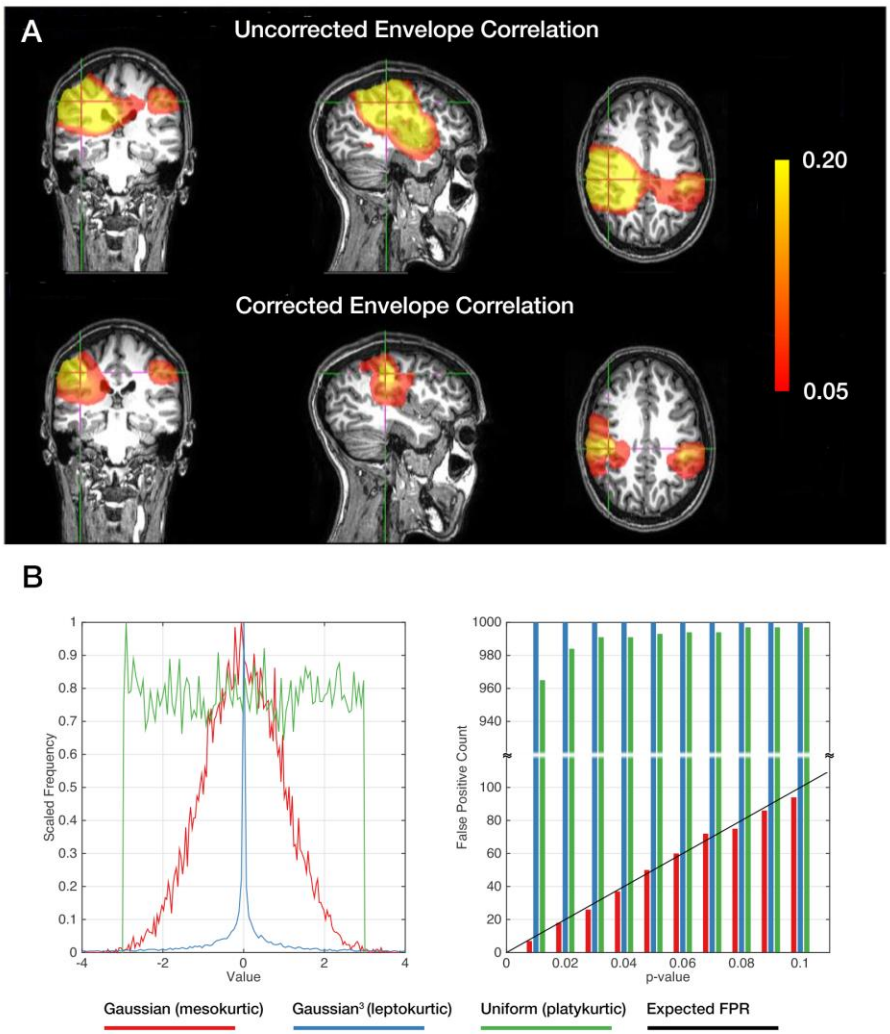

Figure 5: A) An illustration of leakage correction. Top Panel: Envelope correlation in real data between a seed in right motor cortex and all other brain locations, prior to reduction of leakage. Bottom Panel: Envelope correlation for the same data, post leakage reduction. B) Results of a simulation characterising the effectiveness of linear regression as a technique for leakage reduction. Left: The statistical distributions used to generate the underlying independent timecourses S_1 and S_2. *Right: The false positives detected and compared to the theoretical values. Note that only underlying Gaussian distributed data result in agreement between the calculated and theoretical false positive rates and the other distributions return false positives over 96% of the time. Panel A reproduced from (Brookes et al., 2014b).*

Finally, readers should note that the GLM based leakage reduction method is best deployed in pairwise assessments of functional connectivity. It works well for: 1) Calculation of functional connectivity between two spatially separated point locations. 2) Calculation of functional connectivity between two spatially separate voxel clusters (although a multivariate extension is required). 3) Computation of images showing functional connectivity between a seed location or cluster, and all other voxels in the brain (similar to those in Figure 5A). This said, there is a current trend in the neuroimaging literature to move towards "all-to-all" assessment of connectivity. This means that the brain is parcellated into D regions, and electrophysiological timecourses are derived

on a region-by-region basis. Connectivity is then calculated between all region pairs in order to generate a $D \times D$ connectivity matrix (Hillebrand *et al.*, 2012; Tewarie *et al.*, 2014a). In such cases, to avoid leakage problems, no single region timecourse should exhibit any linear zero-phase-lag dependence on any other timecourse. In other words, all D timecourses should be orthogonal to each other, prior to envelope calculation and connectivity estimation. Whilst the pairwise orthogonalisation method could, in principle, be deployed to achieve this (by the regression of every regional timecourse from every other regional timecourse) this brings about significant concerns regarding the order in which the regression is done. In these cases a much more elegant solution is to use the multivariate orthogonalisation procedure proposed recently by (Colclough *et al.*, 2015). This method, based upon Löwdin's symmetrical orthogonalisation (Mayer, 2002; Lowdin, 1950), is able to reduce linear relations between multiple separate timecourses in one calculation. Although this might be considered a more 'aggressive' procedure (i.e. the resulting timecourses are further from the original beamformed data than might be the case for pairwise correction), this technique should be considered the method of choice for inter-regional all-to-all metrics of functional connectivity.

5) ELECTROPHYSIOLOGICAL RSNs AND THEIR RELATIONSHIP TO EXISTING LITERATURE

The pioneering work of (Biswal *et al.*, 1995) showed, that even when the human brain is apparently at rest, meaningful spatial and temporal structure exists in functional imaging data. Specifically, Biswal *et al.* used fMRI to show that, if a blood oxygenation level dependent (BOLD) signal is extracted from left motor cortex, and correlated with voxel timecourses from every other brain region, the areas showing highest correlation were in homologous regions of right sensorimotor cortex. Since this time, the fMRI community have been responsible for a revolution in the way in which researchers approach neuroimaging. Indeed, using similar techniques with seed voxels placed at different cortical locations, multiple networks of connectivity have been robustly extracted from fMRI data (Corbetta, 1998; Raichle *et al.*, 2001; Beckmann *et al.*, 2005; Fox and Raichle, 2007; Fox *et al.*, 2005; Smith *et al.*, 2009; Deco *et al.*, 2011). These networks have been shown to be core to the function of the human brain. Moreover, they are perturbed in a number of different diseases (Schnitzler and Gross, 2005; Kessler *et al.*, 2014; Friston, 1998; Palaniyappan and Liddle, 2012); for example an important hypothesis underlying symptoms of schizophrenia is one of dysconnectivity between regions, and recent work has shown that the salience network (a commonly observed network of functional connectivity in fMRI which incorporates bilateral insula and cingulate cortices) is abnormal (both in structure and function) in schizophrenia patients (Palaniyappan and Liddle, 2012). This is just one of a large number of observations implicating abnormal network structure or

function in diseases ranging from developmental disorders (Haneef *et al.*, 2014; Kessler *et al.*, 2014; Maccotta *et al.*, 2013; Tomasi and Volkow, 2012) to neurodegeneration (Allen *et al.*, 2007; Hacker *et al.*, 2012; Grady *et al.*, 2001; Wang *et al.*, 2007; Hawellek *et al.*, 2011; Leavitt *et al.*, 2014).

The disadvantage of fMRI based network connectivity estimates is that the BOLD response is a haemodynamic process and is therefore an indirect reflection of electrical brain activity. It exhibits limited temporal resolution since the changes in blood flow in response to evoked changes in brain activity, lags the electrical response by ~5-8 s. In addition, artefactual correlation between spatially separate regions could result purely from changes in haemodynamics. For example, changes in heart rate or respiration are known to evoke BOLD changes that are correlated across cortical regions and resemble, to a degree, functional networks (Birn, 2012; Murphy *et al.*, 2013; Tong *et al.*, 2015). It therefore follows that significant advantages can be gained by moving to MEG, which bypasses the haemodynamic response and directly accesses the neural processes that are thought to play a core role in mediating connectivity. Even prior to the growth in functional connectivity analysis, there was a large body of work probing relationships between the haemodynamic response and changes in amplitude of neural oscillations. The primary finding is that good spatial correlation exists between haemodynamic and electrical oscillatory activity, across a broad range of frequencies (Logothetis *et al.*, 2001; Singh *et al.*, 2002; Moradi *et al.*, 2003; Brookes *et al.*, 2005; Mukamel *et al.*, 2005; Winterer *et al.*, 2007; Muthukumaraswamy and Singh, 2008; Zumer *et al.*, 2010; Stevenson *et al.*, 2011; Stevenson *et al.*, 2012). In addition, there is a general trend for a negative relationship between BOLD and low (alpha and beta) frequency oscillations (i.e. when alpha and beta oscillations decrease in power, the BOLD response typically increases) and a concomitant positive correlation between BOLD and high frequency (gamma band) oscillations (Zumer *et al.*, 2010; Mukamel *et al.*, 2005; Hall *et al.*, 2014). These relationships are primarily based on task induced changes in brain activity. However, logically one might hypothesise that similar relationships persist in the resting state, and this has led the MEG community to investigate the relationship between envelope based networks and fMRI derived RSNs.

Figure 6 reproduces (with permission) a selection of results generated by application of the methods described in sections 2, 3 and 4 to MEG data in order to quantify the spatial distribution of networks based on electrophysiological (envelope) connectivity. Figure 6A shows the auditory (left), sensorimotor (centre) and visual (right) RSNs (reproduced from Hipp *et al.*, 2012). In all cases the seed location is shown by the white circle; the colour overlay depicts a leakage corrected map showing regions most highly correlated with the seed envelope; the maximum peak in contralateral

hemisphere is shown by the black cross. These networks show clearly that spatiotemporal structure exists in envelope data. Importantly, the spatial structure is specific to certain oscillatory frequencies and this is shown, for the same auditory, sensorimotor and visual networks, in Figure 6B (again from Hipp *et al.*). The plot shows functional connectivity between hemispheres plotted as a function of frequency band; note that connectivity in the visual network peaks in the alpha band, whereas connectivity in the other two networks peaks in the beta band. Figure 6C again shows a sensorimotor network, identified in an equivalent way and reproduced from Hall and colleagues (Hall *et al.*, 2013); we include this to show the robustness of these spatial maps across a number of studies. Figure 6D shows a spatial comparison of RSNs identified in MEG and fMRI. The default mode, left fronto-parietal, right fronto-parietal and sensorimotor networks are shown and are selected at random from 8 networks observed by (Brookes *et al.*, 2011b) to have a higher than chance correlation with fMRI RSNs. Here, networks have been extracted using temporal ICA rather than seed based correlation. However, the ICA method is applied to the envelopes of neural oscillations and in this way results are equivalent to those in Figures 6A and C. It is clear that a degree of spatial agreement exists between the haemodynamic and electrophysiological findings, however note that source space projection and appropriate compensation for source leakage are key to all of the results presented.

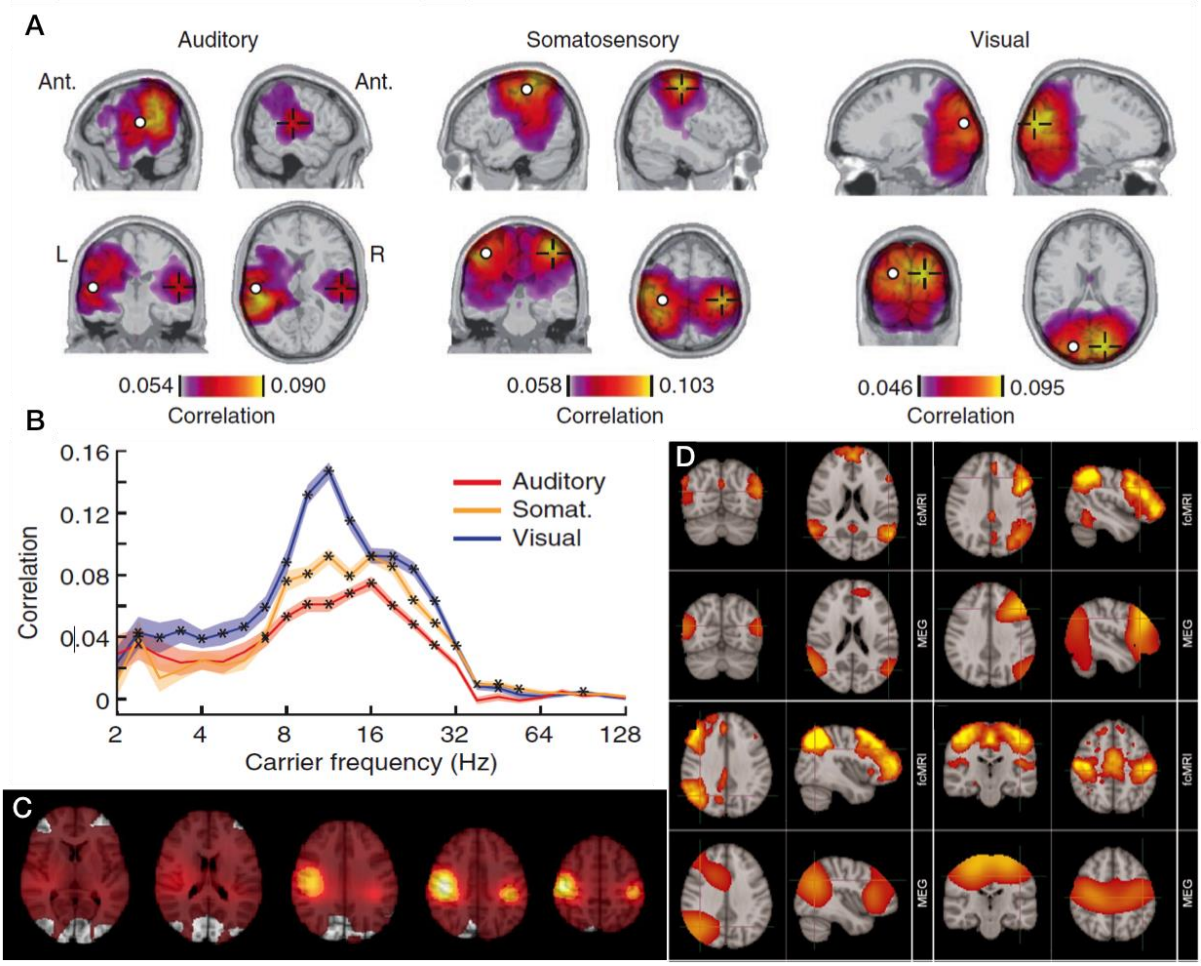

Figure 6: A) Auditory (left), sensorimotor (centre) and visual (right) RSNs. In all cases the seed location is shown by the white circle and the maximum peak in contralateral hemisphere shown by the black cross. B) The spectral signature of functional connectivity. For the three networks in A, connectivity between homologous regions in opposing hemispheres is plotted as a function of frequency, showing clear spectral specificity. C) The sensorimotor network again identified in an equivalent way in Hall et al. D) Shows a direct spatial comparison of RSNs identified in MEG and fMRI. The four networks shown are the default mode, left fronto-parietal, right fronto-parietal and sensorimotor. Panel A and B reproduced from (Hipp et al., 2012), Panel C reproduced from (Hall et al., 2013) and Panel D reproduced from (Brookes et al., 2011b).

The fact that electrophysiological RSNs are in some spatial agreement with fMRI based RSNs is important since it shows that the haemodynamic measurements are not simply a result of correlated haemodynamics that could be driven, for example, by changes in respiration or heart rate. Rather the MEG/fMRI agreement implies that these networks are of neuronal origin. In addition, MEG allows a new dimension for investigation of RSNs: as shown by Figure 6B, RSN structure is not maintained across all frequencies but rather exists within specific (albeit broad) frequency bands. If connectivity between separate pairs of cortical regions is spectrally specific, this represents one way in which, potentially, the brain may build a hierarchical structure of interconnected networks, separated in frequency as well as space. MEG offers a means to probe that complex structure,

although, an important consideration is that the signal to noise ratio (SNR) across different oscillatory frequencies changes with, for example, the high (gamma) bands exhibiting a low SNR compared to the lower frequency alpha and beta range in which connectivity is at maximum. For this reason, the extent to which the spectrally resolved nature of connectivity reflects genuine brain processes, versus simple changes in SNR, is still open to discussion. Early signs suggest this is likely, as recent work from Hipp and Siegel (2015) shows that accounting for SNR reveals frequency specific connections in MEG data ranging from 2-~100 Hz consistently correlating with fMRI-derived topographies rather than just the typical relationship between 8-30 Hz. What is clear is that the large body of published work exploring the neural underpinnings of the haemodynamic response will benefit from these observations. Indeed, the resting state connectome offers a new way in which to investigate the relationship between neuro-electrical and haemodynamic activity. In addition, these results open up a new opportunity to, for the first time, link disease induced perturbations in RSN structure measured in fMRI with altered patterns of neural oscillations, which are a consistent feature of the many neurological disorders. Given the proposed core role of oscillations in mediating functional connectivity, this has the potential to significantly enhance our understanding of the neuro-pathophysiology underlying a range of disorders.

6) FUTURE PROSPECTS: THE DYNAMIC CONNECTOME

The vast majority of RSN studies are based on the assumption that functional connectivity is stationary: that is, connectivity (correlation over time between two regions) is assessed based on an entire experiment, usually comprising several minutes of recorded data. This necessarily implies that functional coupling between two distal regions can be captured by a single parameter. However, the human brain is a dynamic system and the strong likelihood is that mental activity is supported by the formation and dissolution of many transient functional networks, on a rapid timescale. This means that brain networks, and the functional connectivities that define them, are likely to be time dependent. In a paper by Chang and Glover (2010), the authors employed a sliding window analysis, in which connectivity was assessed in many small time windows, that were allowed to shift in time across an fMRI dataset. Their results revealed that the strength of functional connectivity varied markedly, depending on which time window they assessed. Using fast acquisition methods in fMRI, Smith and colleagues (2012) showed that previously established networks were in fact formed from multiple transient components. In addition Allen and colleagues (2014), also using a sliding window analysis, showed significant departures from the spatial structure of canonical RSNs, if transient connectivity was taken into account. These promising results (and many others, see Hutchison *et al.*, 2013 for a review) are in agreement with the hypothesis of a dynamic connectome, and suggest that

future neuroimaging methodologies should be developed to capture transient rather than time averaged connectivity. The millisecond temporal resolution of MEG therefore offers immediate advantages.

A small but growing number of studies are now beginning to show that dynamic assessment of electrophysiological connectivity using MEG implies the existence of significant non-stationarity. In early work, a study by a team lead by de Pasquale (2010) showed that by incorporating non-stationarity into their data processing pipeline, they were able to better resolve the default mode and dorsal attention networks. Brookes and colleagues showed that, in the sensorimotor network, a sliding window analysis showed significant fluctuation in the strength of functional connectivity between motor cortices (Brookes *et al.*, 2011a). This work was extended by Baker and colleagues (2012) who used a similar technique to reveal a bi-stable nature of envelope correlation, with near-zero levels of connectivity interspersed with periods of high connectivity. A further study by Baker et al in 2014 (Baker *et al*., 2014) was able to exploit the excellent temporal resolution of MEG more fully, using a Hidden Markov Model (HMM). This approach, which identifies the points in time at which unique patterns of electrophysiological activity recur, revealed transient (100–200 ms) brain states with spatial topographies similar to RSNs (see Figure 7A). Taken together, these studies begin to demonstrate that within-network functional connectivity is underpinned by coordinated dynamics that fluctuate in time. Importantly, these fluctuations occur at a much more rapid timescale than has previously been envisaged (Baker *et al.*, 2014).

The existence of temporal structure in functional connectivity brings with it considerations for the spatial dynamics of RSNs. Consider Figure 7B which depicts a simple model of a network: at time point 1, regions α and β exhibit a strong connection; at time point 2, regions α and γ exhibit a strong connection. This simple example reflects a transient spatial reorganisation of the network, and illustrates how temporal and spatial analyses can be confounded. Firstly, if connectivity is computed over all time, for example via seed based correlation taking region α as the seed, then this will result in the blurring together of regions β and γ. Secondly, if a sliding window analysis is undertaken between point locations (e.g. between regions α and β) then this captures a dynamic change in functional connectivity (i.e. it results in the blue line in Figure 7Bii), but misses the fact that the spatiotemporal dynamics actually reflect a spatial reorganisation. Thirdly, if cluster metrics are undertaken such that regions β and γ are collapsed together, then this results in a temporal blurring of the dynamics (i.e. the result is the purple dashed line in Figure 7Bii). It therefore follows that methods to capture the true nature of spatiotemporal network dynamics are non-trivial.

Nevertheless methods do exist and an example is given in Figures 7C and 7D. Here, a multivariate technique known as canonical correlation analysis has been employed to calculate functional connectivity between voxel clusters (shown by the green overlay in Figure 7D). The method uses a sliding window, and within each window, the strength of correlation is assessed along with a measure of which voxels maximally contribute to that correlation. The result is effectively a movie showing spatial and spectro-temporal changes in connectivity between the highlighted clusters. In Figure 7C, the time-frequency decomposition of sensorimotor network connectivity in a single subject is shown, where the brighter colours illustrate high levels of connectivity. Note that there is marked temporal structure, with periods of high connectivity interspersed with windows of close to zero connectivity. Note also that in agreement with Figure 6B, the highest levels of coupling occur in the beta frequency band. Figure 7D shows the associated spatial patterns for 7 time windows chosen at random. Note that the spatial signature of sensorimotor network connectivity changes in time with multiple spatially distinct transient networks forming and dissolving depending on the time point (and frequency band) examined (Brookes *et al.*, 2014a; O'Neill *et al.*, 2015).

These assesments of the dynamic connectome are in their infancy. However, results are already beginning to show that novel insights into how brain networks are dynamically recruited in order to support ongoing mental activity can be gained using MEG. In addition, rapidly forming and dissolving connections are being incorporated into computational models of RSNs, with results showing that these transient connections can explain the switching of networks seen in resting state studies (Ponce-Alvarez *et al.*, 2015; Hansen *et al.*, 2015). Given the high level of importance, for both clinical and basic science, attached to static network assessments, it is likely that these dynamic estimations will find equal application in the characterisation of human brain function in health and disease.

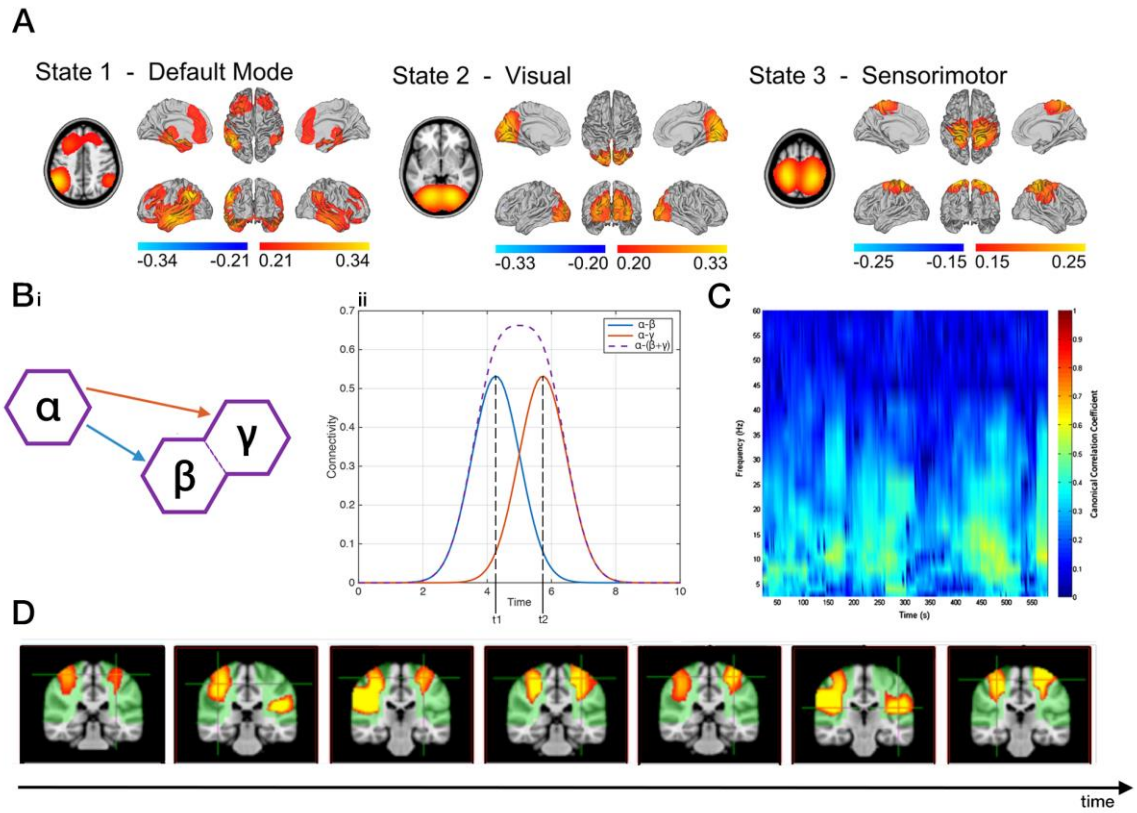

Figure 7: A) Example transient network patterns observed via application of a hidden Markov model to MEG data. These spatial patterns resemble RSNs and were shown to form and dissolve on a time scale of just a few hundred milliseconds, much faster than previously thought. B) A simple model of a functional network. C) Time-frequency decomposition of sensorimotor network connectivity in a single subject, showing the temporal and spectral structure of envelope correlation between clusters in left and right hemispheres. D) The spatial signatures associated with sensorimotor network connectivity shown in C. 7 time windows chosen at random are shown; note the high degree of spatial inhomogeneity across windows. Panel A reproduced from (Baker et al., 2014), Panels C and D reproduced from (Brookes et al., 2014a).

7) CONCLUSION

In this technical review, we have outlined the emerging field of electrophysiological RSN characterisation using envelope based connectivity metrics applied to MEG data. We have shown that MEG has distinct advantages over other methods when characterising network connectivity. Specifically: 1) MEG allows direct measurement of neural oscillations, which are thought to be integral to the mediation of functional coupling. 2) The extremely high temporal resolution of MEG allows for an assessment of network dynamics on a timescale not accessible to fMRI. This said, we have also outlined how the ill-posed MEG inverse problem leads to difficulties in the accurate characterisation of connectivity. This means that source localisation and leakage reduction algorithms are essential if accurate models of connectivity are to result. This is a key point that must be addressed in all future MEG connectivity studies. We have reviewed a growing body of literature suggesting that, envelope based metrics of connectivity show spatial similarity to the established

RSNs observable using fMRI. Finally, we have briefly summarised the emerging topic of dynamic connectivity, highlighting the exciting potential of MEG to uncover the means by which brain networks form and dissolve in support of ongoing moment to moment changes in mental activity. Taken together, the evidence suggests that if appropriate modelling is employed, MEG offers a unique and verifiable means to gain novel insights into brain network coordination. These methods, will be of significant value to elucidate the underlying neural dynamics of brain function in health and disease.

Acknowledgements

We would like to acknowledge the Medical Research Council (MRC) and University of Nottingham (UoN) for funding this work. GCO is funded by an MRC Studentship awarded to UoN. ELB is funded by a UoN Studentship. BAEH is funded by an MRC Doctoral Training Grant (MR/K501086/1). MJB and PKT are funded by an MRC New Investigator Research Grant awarded to MJB (MR/M006301/1). We also acknowledge the MRC MEG Partnership Grant (MR/K005464/1).

References

Allen E A, Damaraju E, Plis S M, Erhardt E B, Eichele T and Calhoun V D 2014 Tracking whole-brain connectivity dynamics in the resting state *Cerebral cortex* **24** 663-76

Allen G, Barnard H, McColl R, Hester A L, Fields J A, Weiner M F, Ringe W K, Lipton A M, Brooker M, McDonald E, Rubin C D and Cullum C M 2007 Reduced hippocampal functional connectivity in Alzheimer disease *Archives of neurology* **64** 1482-7

Baker A P, Brookes M J, Rezek I A, Smith S M, Behrens T, Probert Smith P J and Woolrich M 2014 Fast transient networks in spontaneous human brain activity *eLife* **3** e01867

Baker A P, Luckhoo H, Brookes M J, Smith P and Woolrich M 2012 Investigating the Temporal Dynamics of Resting State Brain Connectivity using Magnetoencephalography. In: *Organization of Human Brain Mapping,* (Beijing, China

Bassett D S, Meyer-Lindenberg A, Achard S, Duke T and Bullmore E 2006 Adaptive reconfiguration of fractal small-world human brain functional networks *Proceedings of the National Academy of Sciences* **103** 19518-23

Bauer M, Stenner M P, Friston K J and Dolan R J 2014 Attentional modulation of alpha/beta and gamma oscillations reflect functionally distinct processes *The Journal of neuroscience : the official journal of the Society for Neuroscience* **34** 16117-25

Beckmann C F, DeLuca M, Devlin J T and Smith S M 2005 Investigations into resting-state connectivity using independent component analysis *Philosophical transactions of the Royal Society of London. Series B, Biological sciences* **360** 1001-13

Berger H 1929 Über das Elektrenkephalogramm des Menschen *Arch Psychiat Nerven* **87** 527-70

Birn R M 2012 The role of physiological noise in resting-state functional connectivity *NeuroImage* **62** 864-70

Biswal B, Yetkin F Z, Haughton V M and Hyde J S 1995 Functional connectivity in the motor cortex of resting human brain using echo-planar MRI *Magnetic resonance in medicine : official journal of the Society of Magnetic Resonance in Medicine / Society of Magnetic Resonance in Medicine* **34** 537-41

Brookes M J, Gibson A M, Hall S D, Furlong P L, Barnes G R, Hillebrand A, Singh K D, Holliday I E, Francis S T and Morris P G 2005 GLM-beamformer method demonstrates stationary field, alpha ERD and gamma ERS co-localisation with fMRI BOLD response in visual cortex *NeuroImage* **26** 302-8

Brookes M J, Hale J R, Zumer J M, Stevenson C M, Francis S T, Barnes G R, Owen J P, Morris P G and Nagarajan S S 2011a Measuring functional connectivity using MEG: methodology and comparison with fcMRI *NeuroImage* **56** 1082-104

Brookes M J, Liddle E B, Hale J R, Woolrich M W, Luckhoo H, Liddle P F and Morris P G 2012a Task induced modulation of neural oscillations in electrophysiological brain networks *NeuroImage* **63** 1918-30

Brookes M J, O'Neill G C, Hall E L, Woolrich M W, Baker A, Palazzo Corner S, Robson S E, Morris P G and Barnes G R 2014a Measuring temporal, spectral and spatial changes in electrophysiological brain network connectivity *NeuroImage* **91** 282-99

Brookes M J, Stevenson C M, Barnes G R, Hillebrand A, Simpson M I, Francis S T and Morris P G 2007 Beamformer reconstruction of correlated sources using a modified source model *NeuroImage* **34** 1454-65

Brookes M J, Vrba J, Robinson S E, Stevenson C M, Peters A M, Barnes G R, Hillebrand A and Morris P G 2008 Optimising experimental design for MEG beamformer imaging *Neuroimage* **39** 1788-802

Brookes M J, Woolrich M, Luckhoo H, Price D, Hale J R, Stephenson M C, Barnes G R, Smith S M and Morris P G 2011b Investigating the electrophysiological basis of resting state networks using magnetoencephalography *Proceedings of the National Academy of Sciences of the United States of America* **108** 16783-8

Brookes M J, Woolrich M W and Barnes G R 2012b Measuring functional connectivity in MEG: a multivariate approach insensitive to linear source leakage *NeuroImage* **63** 910-20

Brookes M J, Woolrich M W and Price D 2014b *Magnetoencephalography,* ed S Supek and C J Aine: Springer Berlin Heidelberg) pp 321-58

Chang C and Glover G H 2010 Time-frequency dynamics of resting-state brain connectivity measured with fMRI *NeuroImage* **50** 81-98

Cohen D 1968 Magnetoencephalography: evidence of magnetic fields produced by alpha-rhythm currents *Science* **161** 784-6

Cohen D 1972 Magnetoencephalography: detection of the brain's electrical activity with a superconducting magnetometer *Science* **175** 664-6

Colclough G L, Brookes M J, Smith S M and Woolrich M W 2015 A symmetric multivariate leakage correction for MEG connectomes *NeuroImage*

Corbetta M 1998 Frontoparietal cortical networks for directing attention and the eye to visual locations: identical, independent, or overlapping neural systems? *Proceedings of the National Academy of Sciences of the United States of America* **95** 831-8

Dalal S S, Sekihara K and Nagarajan S S 2006 Modified beamformers for coherent source region suppression *IEEE transactions on bio-medical engineering* **53** 1357-63

Dale A M, Liu A K, Fischl B R, Buckner R L, Belliveau J W, Lewine J D and Halgren E 2000 Dynamic statistical parametric mapping: combining fMRI and MEG for high-resolution imaging of cortical activity *Neuron* **26** 55-67

de Pasquale F, Della Penna S, Snyder A Z, Lewis C, Mantini D, Marzetti L, Belardinelli P, Ciancetta L, Pizzella V, Romani G L and Corbetta M 2010 Temporal dynamics of spontaneous MEG activity in brain networks *Proceedings of the National Academy of Sciences of the United States of America* **107** 6040-5

Deco G, Jirsa V K and McIntosh A R 2011 Emerging concepts for the dynamical organization of resting-state activity in the brain *Nature reviews. Neuroscience* **12** 43-56
Diwakar M, Tal O, Liu T T, Harrington D L, Srinivasan R, Muzzatti L, Song T, Theilmann R J, Lee R R and Huang M X 2011 Accurate reconstruction of temporal correlation for neuronal sources using the enhanced dual-core MEG beamformer *NeuroImage* **56** 1918-28
Engel A K, Gerloff C, Hilgetag C C and Nolte G 2013 Intrinsic coupling modes: multiscale interactions in ongoing brain activity *Neuron* **80** 867-86
Ewald A, Marzetti L, Zappasodi F, Meinecke F C and Nolte G 2012 Estimating true brain connectivity from EEG/MEG data invariant to linear and static transformations in sensor space *NeuroImage* **60** 476-88
Florin E and Baillet S 2015 The brain's resting-state activity is shaped by synchronized cross-frequency coupling of neural oscillations *NeuroImage* **111** 26-35
Fox M D and Raichle M E 2007 Spontaneous fluctuations in brain activity observed with functional magnetic resonance imaging *Nature reviews. Neuroscience* **8** 700-11
Fox M D, Snyder A Z, Vincent J L, Corbetta M, Van Essen D C and Raichle M E 2005 The human brain is intrinsically organized into dynamic, anticorrelated functional networks *Proceedings of the National Academy of Sciences of the United States of America* **102** 9673-8
Freeman W J 2004 Origin, structure, and role of background EEG activity. Part 1. Analytic amplitude *Clinical neurophysiology : official journal of the International Federation of Clinical Neurophysiology* **115** 2077-88
Friston K J 1998 The disconnection hypothesis *Schizophrenia research* **30** 115-25
Fuchs M, Wagner M, Kohler T and Wischmann H A 1999 Linear and nonlinear current density reconstructions *Journal of clinical neurophysiology : official publication of the American Electroencephalographic Society* **16** 267-95
Gow D W, Jr., Segawa J A, Ahlfors S P and Lin F H 2008 Lexical influences on speech perception: a Granger causality analysis of MEG and EEG source estimates *NeuroImage* **43** 614-23
Grady C L, Furey M L, Pietrini P, Horwitz B and Rapoport S I 2001 Altered brain functional connectivity and impaired short-term memory in Alzheimer's disease *Brain : a journal of neurology* **124** 739-56
Greenblatt R E, Ossadtchi A and Pflieger M E 2005 Local linear estimators for the bioelectromagnetic inverse problem *Ieee T Signal Proces* **53** 3403-12
Gross J, Kujala J, Hamalainen M, Timmermann L, Schnitzler A and Salmelin R 2001 Dynamic imaging of coherent sources: Studying neural interactions in the human brain *Proceedings of the National Academy of Sciences of the United States of America* **98** 694-9
Gross J, Timmermann L, Kujala J, Dirks M, Schmitz F, Salmelin R and Schnitzler A 2002 The neural basis of intermittent motor control in humans *Proceedings of the National Academy of Sciences of the United States of America* **99** 2299-302
Hacker C D, Perlmutter J S, Criswell S R, Ances B M and Snyder A Z 2012 Resting state functional connectivity of the striatum in Parkinson's disease *Brain : a journal of neurology* **135** 3699-711
Hadamard J 1902 Sur les problèmes aux dérivés partielles et leur signification physique *Princeton University Bulletin* **13** 49-52
Hall E L, Robson S E, Morris P G and Brookes M J 2014 The relationship between MEG and fMRI *NeuroImage* **102 Pt 1** 80-91
Hall E L, Woolrich M W, Thomaz C E, Morris P G and Brookes M J 2013 Using variance information in magnetoencephalography measures of functional connectivity *NeuroImage* **67** 203-12
Hämäläinen M, Hari R, Ilmoniemi R, Knuutila J and Lounasmaa O 1993 Magnetoencephalography---theory, instrumentation, and applications to noninvasive studies of the working human brain *Reviews of Modern Physics* **65** 413-97

Hamalainen M S and Ilmoniemi R J 1994 Interpreting magnetic fields of the brain: minimum norm estimates *Medical & biological engineering & computing* **32** 35-42
Haneef Z, Lenartowicz A, Yeh H J, Levin H S, Engel J, Jr. and Stern J M 2014 Functional connectivity of hippocampal networks in temporal lobe epilepsy *Epilepsia* **55** 137-45
Hansen E C, Battaglia D, Spiegler A, Deco G and Jirsa V K 2015 Functional connectivity dynamics: modeling the switching behavior of the resting state *NeuroImage* **105** 525-35
Hawellek D J, Hipp J F, Lewis C M, Corbetta M and Engel A K 2011 Increased functional connectivity indicates the severity of cognitive impairment in multiple sclerosis *Proceedings of the National Academy of Sciences of the United States of America* **108** 19066-71
Hillebrand A, Barnes G R, Bosboom J L, Berendse H W and Stam C J 2012 Frequency-dependent functional connectivity within resting-state networks: an atlas-based MEG beamformer solution *NeuroImage* **59** 3909-21
Hillebrand A, Singh K D, Holliday I E, Furlong P L and Barnes G R 2005 A new approach to neuroimaging with magnetoencephalography *Human brain mapping* **25** 199-211
Hipp J F, Hawellek D J, Corbetta M, Siegel M and Engel A K 2012 Large-scale cortical correlation structure of spontaneous oscillatory activity *Nature neuroscience* **15** 884-90
Hipp J F and Siegel M 2015 BOLD fMRI Correlation Reflects Frequency-Specific Neuronal Correlation *Current biology : CB* **25** 1368-74
Hutchison R M, Womelsdorf T, Allen E A, Bandettini P A, Calhoun V D, Corbetta M, Della Penna S, Duyn J H, Glover G H, Gonzalez-Castillo J, Handwerker D A, Keilholz S, Kiviniemi V, Leopold D A, de Pasquale F, Sporns O, Walter M and Chang C 2013 Dynamic functional connectivity: promise, issues, and interpretations *NeuroImage* **80** 360-78
Ioannides A A, Liu L C, Kwapien J, Drozdz S and Streit M 2000 Coupling of regional activations in a human brain during an object and face affect recognition task *Human brain mapping* **11** 77-92
Jerbi K, Lachaux J P, N'Diaye K, Pantazis D, Leahy R M, Garnero L and Baillet S 2007 Coherent neural representation of hand speed in humans revealed by MEG imaging *Proceedings of the National Academy of Sciences of the United States of America* **104** 7676-81
Kessler D, Angstadt M, Welsh R C and Sripada C 2014 Modality-Spanning Deficits in Attention-Deficit/Hyperactivity Disorder in Functional Networks, Gray Matter, and White Matter *The Journal of Neuroscience* **34** 16555-66
Kiebel S J, Tallon-Baudry C and Friston K J 2005 Parametric analysis of oscillatory activity as measured with EEG/MEG *Human brain mapping* **26** 170-7
Le Van Quyen M, Foucher J, Lachaux J-P, Rodriguez E, Lutz A, Martinerie J and Varela F J 2001 Comparison of Hilbert transform and wavelet methods for the analysis of neuronal synchrony *Journal of neuroscience methods* **111** 83-98
Leavitt V, Wylie G, Girgis P, DeLuca J and Chiaravalloti N 2014 Increased functional connectivity within memory networks following memory rehabilitation in multiple sclerosis *Brain Imaging and Behavior* **8** 394-402
Liu Z, Fukunaga M, de Zwart J A and Duyn J H 2010 Large-scale spontaneous fluctuations and correlations in brain electrical activity observed with magnetoencephalography *NeuroImage* **51** 102-11
Logothetis N K, Pauls J, Augath M, Trinath T and Oeltermann A 2001 Neurophysiological investigation of the basis of the fMRI signal *Nature* **412** 150-7
Lowdin P O 1950 On the Non-Orthogonality Problem Connected with the Use of Atomic Wave Functions in the Theory of Molecules and Crystals *Journal of Chemical Physics* **18** 365-75
Luckhoo H, Hale J R, Stokes M G, Nobre A C, Morris P G, Brookes M J and Woolrich M W 2012 Inferring task-related networks using independent component analysis in magnetoencephalography *NeuroImage* **62** 530-41

Maccotta L, He B J, Snyder A Z, Eisenman L N, Benzinger T L, Ances B M, Corbetta M and Hogan R E 2013 Impaired and facilitated functional networks in temporal lobe epilepsy *NeuroImage. Clinical* **2** 862-72
Maldjian J A, Davenport E M and Whitlow C T 2014 Graph theoretical analysis of resting-state MEG data: Identifying interhemispheric connectivity and the default mode *NeuroImage* **96** 88-94
Marzetti L, Della Penna S, Snyder A Z, Pizzella V, Nolte G, de Pasquale F, Romani G L and Corbetta M 2013 Frequency specific interactions of MEG resting state activity within and across brain networks as revealed by the multivariate interaction measure *NeuroImage* **79** 172-83
Mayer I 2002 On Lowdin's method of symmetric orthogonalization *Int J Quantum Chem* **90** 63-5
Moradi F, Liu L C, Cheng K, Waggoner R A, Tanaka K and Ioannides A A 2003 Consistent and precise localization of brain activity in human primary visual cortex by MEG and fMRI *NeuroImage* **18** 595-609
Mukamel R, Gelbard H, Arieli A, Hasson U, Fried I and Malach R 2005 Coupling between neuronal firing, field potentials, and FMRI in human auditory cortex *Science* **309** 951-4
Murphy K, Birn R M and Bandettini P A 2013 Resting-state fMRI confounds and cleanup *NeuroImage* **80** 349-59
Muthukumaraswamy S D and Singh K D 2008 Spatiotemporal frequency tuning of BOLD and gamma band MEG responses compared in primary visual cortex *NeuroImage* **40** 1552-60
Nolte G, Bai O, Wheaton L, Mari Z, Vorbach S and Hallett M 2004 Identifying true brain interaction from EEG data using the imaginary part of coherency *Clinical neurophysiology : official journal of the International Federation of Clinical Neurophysiology* **115** 2292-307
Nolte G, Ziehe A, Nikulin V V, Schlogl A, Kramer N, Brismar T and Muller K R 2008 Robustly estimating the flow direction of information in complex physical systems *Physical review letters* **100** 234101
Nunez P L and Srinivasan R 2006 *Electric fields of the brain: the neurophysics of EEG*: Oxford university press)
O'Neill G C, Bauer M, Woolrich M W, Morris P G, Barnes G R and Brookes M J 2015 Dynamic recruitment of resting state sub-networks *NeuroImage* **115** 85-95
O'Neill G C, Hall E, Palazzo Corner S, Morris P G and Brookes M J 2013 A Comparison of Beamformer and Minimim Norm Soultions for MEG Network Connectivity Mapping. In: *Organization of Human Brain Mapping,* (Seattle, WA
Palaniyappan L and Liddle P F 2012 Does the salience network play a cardinal role in psychosis? An emerging hypothesis of insular dysfunction *Journal of psychiatry & neuroscience : JPN* **37** 17-27
Palva J M, Monto S, Kulashekhar S and Palva S 2010 Neuronal synchrony reveals working memory networks and predicts individual memory capacity *Proceedings of the National Academy of Sciences of the United States of America* **107** 7580-5
Pascual-Marqui R D 2002 Standardized low-resolution brain electromagnetic tomography (sLORETA): technical details *Methods and findings in experimental and clinical pharmacology* **24 Suppl D** 5-12
Ponce-Alvarez A, Deco G, Hagmann P, Romani G L, Mantini D and Corbetta M 2015 Resting-state temporal synchronization networks emerge from connectivity topology and heterogeneity *PLoS computational biology* **11** e1004100
Popescu M, Popescu E A, Chan T, Blunt S D and Lewine J D 2008 Spatio-temporal reconstruction of bilateral auditory steady-state responses using MEG beamformers *IEEE transactions on bio-medical engineering* **55** 1092-102
Prendergast G, Green G G and Hymers M 2013 A robust implementation of a kurtosis beamformer for the accurate identification of epileptogenic foci *Clinical neurophysiology : official journal of the International Federation of Clinical Neurophysiology* **124** 658-66

Prichard D and Theiler J 1994 Generating Surrogate Data for Time-Series with Several Simultaneously Measured Variables *Physical review letters* **73** 951-4
Puts N A, Edden R A, Evans C J, McGlone F and McGonigle D J 2011 Regionally specific human GABA concentration correlates with tactile discrimination thresholds *The Journal of neuroscience : the official journal of the Society for Neuroscience* **31** 16556-60
Raichle M E, MacLeod A M, Snyder A Z, Powers W J, Gusnard D A and Shulman G L 2001 A default mode of brain function *Proceedings of the National Academy of Sciences of the United States of America* **98** 676-82
Robinson S and Vrba J 1998 Functional neuroimaging by synthetic aperture magnetometry (SAM) *Recent advances in biomagnetism* 302-5
Schnitzler A and Gross J 2005 Functional connectivity analysis in magnetoencephalography *International review of neurobiology* **68** 173-95
Schoffelen J M and Gross J 2009 Source connectivity analysis with MEG and EEG *Human brain mapping* **30** 1857-65
Scholvinck M L, Leopold D A, Brookes M J and Khader P H 2013 The contribution of electrophysiology to functional connectivity mapping *NeuroImage* **80** 297-306
Sekihara K, Hild K E and Nagarajan S S 2006 A novel adaptive beamformer for MEG source reconstruction effective when large background brain activities exist *Biomedical Engineering, IEEE Transactions on* **53** 1755-64
Sekihara K and Nagarajan S S 2008 *Adaptive Spatial Filters for Electromagnetic Brain Imaging*: Springer Berlin Heidelberg)
Sekihara K, Nagarajan S S, Poeppel D, Marantz A and Miyashita Y 2001 Reconstructing spatio-temporal activities of neural sources using an MEG vector beamformer technique *Biomedical Engineering, IEEE Transactions on* **48** 760-71
Singer W 1999 Neuronal synchrony: a versatile code for the definition of relations? *Neuron* **24** 49-65, 111-25
Singh K D, Barnes G R, Hillebrand A, Forde E M and Williams A L 2002 Task-related changes in cortical synchronization are spatially coincident with the hemodynamic response *NeuroImage* **16** 103-14
Smith S M, Fox P T, Miller K L, Glahn D C, Fox P M, Mackay C E, Filippini N, Watkins K E, Toro R, Laird A R and Beckmann C F 2009 Correspondence of the brain's functional architecture during activation and rest *Proceedings of the National Academy of Sciences of the United States of America* **106** 13040-5
Smith S M, Miller K L, Moeller S, Xu J, Auerbach E J, Woolrich M W, Beckmann C F, Jenkinson M, Andersson J, Glasser M F, Van Essen D C, Feinberg D A, Yacoub E S and Ugurbil K 2012 Temporally-independent functional modes of spontaneous brain activity *Proceedings of the National Academy of Sciences of the United States of America* **109** 3131-6
Stam C J 2004 Functional connectivity patterns of human magnetoencephalographic recordings: a 'small-world'network? *Neuroscience letters* **355** 25-8
Stam C J, Nolte G and Daffertshofer A 2007 Phase lag index: assessment of functional connectivity from multi channel EEG and MEG with diminished bias from common sources *Human brain mapping* **28** 1178-93
Stevenson C M, Brookes M J and Morris P G 2011 beta-Band correlates of the fMRI BOLD response *Human brain mapping* **32** 182-97
Stevenson C M, Wang F, Brookes M J, Zumer J M, Francis S T and Morris P G 2012 Paired pulse depression in the somatosensory cortex: associations between MEG and BOLD fMRI *NeuroImage* **59** 2722-32
Stockwell R G, Mansinha L and Lowe R P 1996 Localization of the complex spectrum: The S transform *Ieee T Signal Proces* **44** 998-1001
Tass P, Rosenblum M G, Weule J, Kurths J, Pikovsky A, Volkmann J, Schnitzler A and Freund H J 1998 Detection of n:m Phase Locking from Noisy Data: Application to Magnetoencephalography *Physical review letters* **81** 3291-4
Tewarie P, Hillebrand A, van Dellen E, Schoonheim M M, Barkhof F, Polman C H, Beaulieu C, Gong G, van Dijk B W and Stam C J 2014a Structural degree predicts

functional network connectivity: a multimodal resting-state fMRI and MEG study *NeuroImage* **97** 296-307
Tewarie P, Schoonheim M M, Stam C J, van der Meer M L, van Dijk B W, Barkhof F, Polman C H and Hillebrand A 2013 Cognitive and clinical dysfunction, altered MEG resting-state networks and thalamic atrophy in multiple sclerosis *PloS one* **8** e69318
Tewarie P, Steenwijk M D, Tijms B M, Daams M, Balk L J, Stam C J, Uitdehaag B M, Polman C H, Geurts J J, Barkhof F, Pouwels P J, Vrenken H and Hillebrand A 2014b Disruption of structural and functional networks in long-standing multiple sclerosis *Human brain mapping* **35** 5946-61
Tomasi D and Volkow N D 2012 Abnormal functional connectivity in children with attention-deficit/hyperactivity disorder *Biological psychiatry* **71** 443-50
Tong Y, Hocke L M, Fan X, Janes A C and Frederick B 2015 Can apparent resting state connectivity arise from systemic fluctuations? *Frontiers in human neuroscience* **9** 285
Troebinger L, Lopez J D, Lutti A, Bestmann S and Barnes G 2014 Discrimination of cortical laminae using MEG *NeuroImage* **102 Pt 2** 885-93
Van Drongelen W, Yuchtman M, Van Veen B and Van Huffelen A 1996 A spatial filtering technique to detect and localize multiple sources in the brain *Brain Topography* **9** 39-49
Van Veen B D, van Drongelen W, Yuchtman M and Suzuki A 1997 Localization of brain electrical activity via linearly constrained minimum variance spatial filtering *Biomedical Engineering, IEEE Transactions on* **44** 867-80
Vinck M, Oostenveld R, van Wingerden M, Battaglia F and Pennartz C M 2011 An improved index of phase-synchronization for electrophysiological data in the presence of volume-conduction, noise and sample-size bias *NeuroImage* **55** 1548-65
Wang K, Liang M, Wang L, Tian L, Zhang X, Li K and Jiang T 2007 Altered functional connectivity in early Alzheimer's disease: a resting-state fMRI study *Human brain mapping* **28** 967-78
Wens V, Bourguignon M, Goldman S, Marty B, Op de Beeck M, Clumeck C, Mary A, Peigneux P, Van Bogaert P, Brookes M J and De Tiege X 2014a Inter- and Intra-Subject Variability of Neuromagnetic Resting State Networks *Brain topography*
Wens V, Mary A, Bourguignon M, Goldman S, Marty B, Beeck M O, Bogaert P V, Peigneux P and Tiege X D 2014b About the electrophysiological basis of resting state networks *Clinical neurophysiology : official journal of the International Federation of Clinical Neurophysiology* **125** 1711-3
Wibral M, Lizier J T, Vogler S, Priesemann V and Galuske R 2014 Local active information storage as a tool to understand distributed neural information processing *Frontiers in neuroinformatics* **8** 1
Winterer G, Carver F W, Musso F, Mattay V, Weinberger D R and Coppola R 2007 Complex relationship between BOLD signal and synchronization/desynchronization of human brain MEG oscillations *Human brain mapping* **28** 805-16
Zimmerman J E, Thiene P and Harding J T 1970 Design and Operation of Stable Rf-Biased Superconducting Point-Contact Quantum Devices, and a Note on Properties of Perfectly Clean Metal Contacts *J Appl Phys* **41** 1572-&
Zumer J M, Brookes M J, Stevenson C M, Francis S T and Morris P G 2010 Relating BOLD fMRI and neural oscillations through convolution and optimal linear weighting *NeuroImage* **49** 1479-89